Nanoscale

Accepted Manuscript

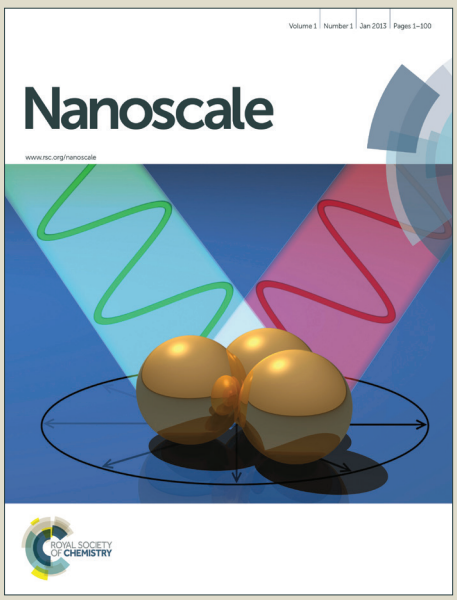

ROYAL SOCIETY OF CHEMISTRY

www.rsc.org/nanoscale

Journal Name

RSCPublishing

ARTICLE

The Spherical Core-shell Magnetic Particles Constructed by Main-chain Palladium *N*-Heterocyclic Carbenes

Huaixia Zhao,[a,b] Liuyi Li,[a] Jinyun Wang [a] and Ruihu Wang*[a]

Cite this: DOI: 10.1039/xoxxoooooox

Received ooth January 2012,
Accepted ooth January 2012

DOI: 10.1039/xoxxoooooox

www.rsc.org/

The encapsulation of functional species on magnetic core is a facile approach for the synthesis of core-shell magnetic materials, surface encapsulating matrices play crucial roles in regulating their properties and applications. In this work, two core-shell palladium *N*-heterocyclic carbene (NHC) particles (Fe_3O_4@PNP1 and Fe_3O_4@PNP2) were prepared by one-pot reaction of semi-rigid tripodal imidazolium salts and palladium acetate in the presence of magnetite nanoparticles. The magnetite nanoparticles are encapsulated inside main-chain palladium NHC matrices as the core. The conjugated effects of triphenyltriazine and triphenylbenzene in the imidazolium salts have important effects on their physical properties and catalytic performances. Fe_3O_4@PNP2 shows better recyclability than Fe_3O_4@PNP1. Unexpectedly, Pd(II) is well maintained after six consecutive catalytic runs in Fe_3O_4@PNP2, while Pd(0) and Pd(II) coexist in Fe_3O_4@PNP1 under the same conditions, the morphologies of these spherical core-shell particles have no significant variation after six consecutive catalytic runs.

Introduction

Nanometer- and micrometer-sized spherical particles have attracted continuous attention in catalysis, drug delivery, gas storage, material science.[1-3] Various methods have been developed for controllable synthesis of spherical inorganic particles, organic particles and coordination polymer particles[3]. Among them, metal-organic coordination polymer particles are one type of promising spherical materials, which are formed through coordination-directed assembly of metal ions and polydentate organic ligands.[4] A high density of molecule-based functionalities can be readily introduced into the spheres through judicial selection of transition metal connectors and predefined functional organic building blocks, but reversible nature of metal-coordination chemistry usually makes them unstable enough in most of liquid-phase catalytic reactions. In comparison with functional metal-organic coordination polymer particles, *N*-heterocyclic carbene (NHC)-based organometallic polymers are more attractive in catalysis owing to remarkable similarity to electron-rich phosphine ligands and strong binding ability with metal ions.[5] Recently, several main-chain palladium NHC particles have been reported, and the excellent catalytic performances have been shown in palladium-catalyzed organic reactions.[6] The catalytic performances of such particles are closely related to chemical or physical properties of the particle surface, and the catalytic active centers inside backbone of these materials are difficult for reaction substrates to access. The inefficient utilization of interior palladium contents decreases their catalytic efficiency and increases the cost of the catalysts. In addition, tedious filtration or centrifugation is usually required for recovery and recycling of the catalysts.

The spherical particles of core-shell structures are of great interest in heterogeneous catalysis.[7] The use of less expensive materials as the core of spherical particles may greatly save the cost of precious metal catalysts. Superparamagnetic nanoparticles (NPs) are one of promising cores in clean and sustainable chemistry owing to their advantages, such as low toxicity, inexpensiveness, ready availability and facile retrievability.[8-10] The resulting core-shell magnetic particles can be easily separated with the help of external magnetic

field, and the properties and applications can be flexibly manipulated by their surface modification. However, the spherical magnetic particles are usually prepared by grafting functional groups to magnetic cores.[8,9] In contrast, the encapsulation of functional species on exterior magnetic core is a more straightforward method for the controllable synthesis of core-shell materials. Although several materials encapsulating superparamagnetic NPs have been reported,[10] the exploration of spherical core-shell magnetic particles covering iron oxide NPs are still rare.[11] To our best knowledge, the use of main-chain palladium NHC particles as encapsulating matrices has not been reported hitherto. In our continuous effort to develop highly efficient heterogeneous catalytic systems,[12] herein, we report a simple one-pot synthesis of magnetically separable palladium NHC particles (Fe_3O_4@PNP1 and Fe_3O_4@PNP2) through efficient encapsulation of superparamagnetic NPs by main-chain palladium NHC polymers.

Experimental details

General Methods

Tris-2,4,6-(4'-(chloromethyl)phenyl)-1,3,5-triazine[16] and tris-1,3,5-(4'-(chloromethyl)phenyl)benzene[17] were synthesized according to literature methods, other chemicals and solvents were commercially available and were used as received. ^{1}H and ^{13}C NMR spectra were recorded on a Bruker AVANCE III NMR spectrometer at 400 and 100 MHz, respectively, using tetramethylsilane (TMS) as an internal standard. Solid-state ^{13}C NMR was performed on a Bruker SB Avance III 500 MHz spectrometer with a 4 mm double-resonance MAS probe, a sample spinning rate of 7.0 kHz, a contact time of 2 ms and pulse delay of 5 s. IR spectra were recorded with KBr pellets using Perkin-Elmer Instrument. Thermogravimetric-mass spectrometric (TG-MS) analysis was carried out on NETZSCH STA 449C spectrometer by heating samples from 35 to 800 ºC in a dynamic nitrogen atmosphere with a heating rate of 10 °C·min^{-1}. Field-emission scanning electron microscopy (SEM) and SEM elementary mapping images were performed on a JEOL JSM-7500F electron microscope, operated at an accelerating voltage of 3.0 kV. Transmission electron microscope (TEM) images were obtained with TECNAI G^2 F20 electron microscope. The magnetic susceptibility data were collected with a Quantum Design MPMS model 6000 magnetometer at 300K in a magnetic field from -10 to +10 Oe. Powder XRD patterns were obtained using a Philips X'Pert-MPD diffractometer with CuKα radiation (λ = 1.54056 Å). X-ray photoelectron spectroscopy (XPS) measurements were performed on a Thermo ESCALAB 250 spectrometer, using non-monochromatic Al Kα x-rays as the excitation source and choosing C 1s (284.6 eV) as the reference line. Inductively coupled plasma (ICP) analyses were performed on Jobin Yvon Ultima2 spectrometer. Gas chromatography (GC) was performed on a Shimadzu GC-2014 equipped with a capillary column (RTX-5, 30 m×0.25 μm) using a flame ionization detector. Elemental analyses were performed on an Elementar Vario MICRO Elemental analyzer.

Calculation method

All calculations were implemented in Gaussian 03 program.[18] The density functional theory (DFT) method at the hybrid Becke three-parameter Lee-Yang-Parr (B3LYP)[19] functional level was used to study the complexes TIPT-Cl and TIPB-Cl. The geometrical structures were initially optimized. During the calculation processes, the convergent values of maximum force, root-mean-square (RMS) force, maximum displacement, and RMS displacement were set by default. Then, the natural bond orbital (NBO) analysis[20] was implemented in complex TIPT-Cl. In these calculations, the all-electron basis set of 6-31G* was used. Visualization of the formed H bond and electrostatic potential mapped onto electron desnsity surface were performed by GaussView.

Preparation of TIPT-Cl

2,4,6-Tris(4'-(chloromethyl)phenyl)-1,3,5-triazine (0.91 g, 2.0 mmol) and 1-methyl-1H-imidazole (2.4 mL, 30 mmol) were added into DMF (100 mL). The reaction mixture was stirred at 100ºC for 48 h, the resultant white precipitate was filtered, washed with DMF and CH_2Cl_2, and dried under vacuum. Yield: 1.01g (72%). ^{1}H NMR (DMSO-d_6): δ 9.46 (s, 3H), 8.76 (d, J = 7.56 Hz, 6H), 7.91 (s, 3H), 7.80 (s, 3H), 7.72 (d, J = 7.80 Hz, 6H), 5.64 (s, 6H), 3.90 (s, 9H); ^{13}C NMR (DMSO-d_6): δ 171.2, 140.4, 137.5, 136.0, 129.8, 129.4, 124.6, 123.0, 51.9, 36.4. IR (KBr, cm^{-1}): 1658(w), 1587(w), 1521(s),

1453(w), 1420(w), 1377(m), 1194(m), 1165(m), 1022(m), 955(w), 878(w), 854(w), 825(m), 796(m), 758(m), 705(w), 662(w), 619(m), 504(w). Elemental analysis calcd (%) for $C_{36}H_{36}Cl_3N_9 \cdot 4.5H_2O$: C, 55.28; H, 5.80; N, 16.12; found: C, 55.24; H, 5.77; N, 16.53

Preparation of TIPB-Cl

TIPB-Cl was synthesized by the same procedure as that of TIPT-Cl except that 2,4,6-tris(4'-(chloromethyl)phenyl)-1,3,5-triazine was replaced by 1,3,5-tris(4'-(chloromethyl)phenyl)benzene. Yield: 0.91g (65%). ^{1}H NMR (DMSO-d_6): δ 9.50 (s, 3H), 7.92 (t, J = 7.72 Hz, 12H), 7.78 (s, 3H), 7.61 (d, J = 8.04 Hz, 6H), 5.54 (s, 6H), 3.90 (s, 9H); ^{13}C NMR (DMSO-d_6): δ 141.5, 140.7, 137.3, 135.1, 129.6, 128.2, 125.2, 124.5, 122.8, 51.8, 36.4. IR (KBr, cm^{-1}): 1635(m), 1560(m), 1510(m), 1452(w), 1396(m), 1361(w), 1330(w), 1282(w), 1211(w), 1165(s), 1018(w), 837(m), 785(m), 756(m), 711(w), 663(w), 519(w). Elemental analysis calcd (%) for $C_{39}H_{39}Cl_3N_6 \cdot 4.5H_2O$: C, 60.12; H, 6.21; N, 10.79; found: C, 60.46; H, 6.66; N, 10.51.

Preparation of PNP1

A solution of $Pd(OAc)_2$ (10 mg, 0.045 mmol) in DMF (1 mL) was injected to a solution of TIPT-Cl (21 mg, 0.03 mmol) in DMF (7 mL) at 110 ^{o}C. The reaction mixture was stirred at this temperature for 5 h to give yellow precipitate. After cooling to room temperature, the solid was collected by centrifugation, washed with DMF, CH_2Cl_2 and diethyl ether, and then dried under vacuum. Yield: 0.012g (46%). IR (KBr, cm^{-1}): 1612(w), 1584(m), 1517(s), 1462(w), 1415(w), 1368(s), 1235(w), 1184(w), 1151(w), 1112(w), 1017(m), 798(m), 775(m), 739(m), 688(w), 609(w), 512(w). Elemental analysis calcd (%) for $C_{36}H_{36}Br_3N_9Pd_{1.5}$: C, 43.50; H, 3.65; N, 12.68; found: C, 45.76; H, 4.79; N, 13.52.

Preparation of PNP2

The same procedure as that of PNP1 was used except that TIPT-Cl was replaced by TIPB-Cl. Yellow PNP2 was obtained in 30% yield. IR (KBr, cm^{-1}): 1717(w), 1559(s), 1571(s), 1513(s), 1465(s), 1443(s), 1390(s), 1358(w), 1232(m), 1153(w), 1117(w), 1084(w), 1017(w), 818(m), 774(m), 726(m), 693(m), 610(w), 521(w). Elemental analysis calcd (%) for $C_{39}H_{39}Br_3N_6Pd_{1.5}$: C, 47.26; H, 3.97; N, 8.48; found: C, 50.00; H, 5.43; N, 8.98.

Preparation of Fe_3O_4@PNP1

A solution of $Pd(OAc)_2$ (100 mg, 0.45 mmol) in DMF (10mL) was injected to a solution of TIPT-Cl (210 mg, 0.30 mmol) in DMF with toluene-dispersed Fe_3O_4 NPs (70 mL) under sonication at 100 ^{o}C. The reaction mixture was sonicated at this temperature for 1 h，then stirred in oil for 4h to give rise to brown precipitate. After cooling to room temperature, the solid was collected by a permanent magnet, washed with DMF, CH_2Cl_2 and diethyl ether, and then dried under vacuum. Yield: 0.14g (37%). IR (KBr, cm^{-1}): 1616(w), 1585(w), 1520(s), 1463(w), 1420(w), 1367(m), 1236(w), 1185(w), 1151(w), 1108(w), 1017(m), 950(w), 873(w), 796(m), 772(w), 734(w), 682(w), 610(w), 514(w).

Preparation of Fe_3O_4@PNP2

The same procedure as that of Fe_3O_4@PNP1 was used except that TIPT-Cl was replaced by TIPB-Cl. Brown Fe_3O_4@PNP2 was obtained in 35% yield. IR (KBr, cm^{-1}): 1717(w), 1659(s), 1601(m), 1573(m), 1516(m), 1463(s), 1396(s), 1362(w), 1236(m), 1190(w), 1123(w), 1084(w), 1017(w), 821(m), 778(m), 729(w), 691(w), 610(w), 514(w).

General procedures for Suzuki-Miyaura cross-coupling reaction

A 25 mL reactor equipped with a screw cap was charged with 4-bromoacetophenone (0.5 mmol), phenylboronic acid (0.75 mmol), K_2CO_3 (1.0 mmol) and palladium NHC particles (1 mol% Pd) in H_2O (1.0 mL) and EtOH (2.0 mL). The reaction mixture was stirred at 25 ^{o}C for 1h. The resultant mixture was extracted with ethyl acetate (3 x 5 mL) and the conversion was determined by GC.

Recyclability test of Fe_3O_4@PNP

A mixture of 4-bromoacetophenone (2.0 mmol), phenylboronic acid (3.0 mmol), Fe_3O_4@PNP (1 mol% Pd) and K_2CO_3 (4.0 mmol) in H_2O (4.0 mL) and EtOH (8.0 mL) was stirred at 25 ^{o}C for 1h. After the completion of the reaction, the crude product was extracted with ethyl acetate (3 x 10 mL) and the conversion was determined by GC, followed by the addition of acetone. The palladium NHC particles were then separated by a permanent magnet, washed with H_2O, acetone and Et_2O to remove residual product, and then dried and subjected to the next run.

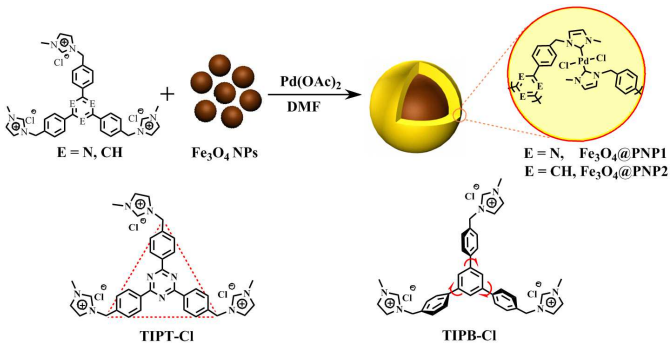

Scheme 1. General synthetic illustration of Fe_3O_4@PNP1 and Fe_3O_4@PNP2.

Results and discussion

Imidazolium-based ionic salts are well known to be excellent precursors of metal NHCs, and main-chain palladium NHC particles are usually prepared through a concerted process of deprotonation of bis- or poly-imidazolium salts and subsequent metalation of palladium(II).[13] 2,4,6-Tris[4-(1-methyl-imidazolium-3-methylene)phenyl]-1,3,5-triazine trichloride (TIPT-Cl) and 1,3,5-tris[4-(1-methyl-imidazolium-3-methylene)phenyl]-benzene trichloride (TIPB-Cl) were readily prepared through quaternization of 2,4,6-tris(4'-chloromethylphenyl)-1,3,5-triazine and tris-1,3,5-(4'-chloromethylphenyl)benzene with 1-methyl-1H-imidazole in DMF, respectively. In the tripodal imidazolium salts, three imidazolium groups are connected to the central triphenyltriazine or triphenylbenzene *via* flexible methylene group (Scheme 1), which may freely twist in the formation of palladium NHC complexes. As well-known, 1,3,5-triazine ring possess stronger electron affinity than phenyl ring, the negatively charged nitrogen atoms may act as electron donor to form hydrogen bond with C–H bonds on the peripheral rings (Figure S1), so the covalent linkage with three phenyl rings is apt to induce an effective conjugation, resulting in the rigidity of the aromatic planes in TIPT-Cl. However, the repulsions between C-H bonds of the central phenyl ring and those on the peripheral phenyl rings may prevent the planarity of aromatic rings in TIPB-Cl.[14] As a result, triphenylbenzene in TIPB-Cl possesses better flexibility owing to rotational freedom between phenyl rings (Figure 1). These results were further confirmed by the theoretical calculation of the total energy versus the dihedral angle between the central ring and peripheral phenyl rings. In TIPT-Cl, the total energy is the lowest when their dihedral angle is zero, while TIPB-Cl with the dihedral angle of 38.85° possesses the lowest total energy.

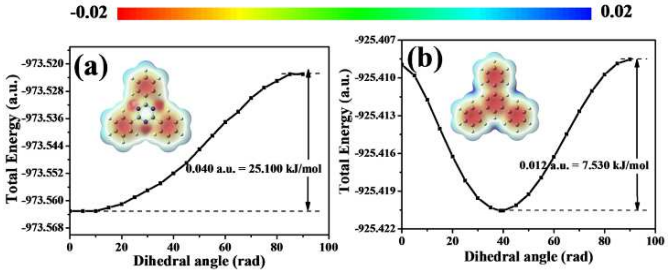

Figure 1. The total energy versus the dihedral angle between central ring and peripheral phenyl rings and ESP mapped onto electron density surface of TIPT-Cl (a) and TIPB-Cl (b).

The reaction of TIPT-Cl and TIPB-Cl with 1.5 equivalent of palladium acetate in DMF at 110 °C generated spherical PNP1 and PNP2, respectively. Their average diameters are around 350 and 600 nm, respectively (Figure 2a and b). When solvent volume is decreased to half of original volume in the synthesis of PNP2, larger spherical palladium NHC particles with average size around 1.5 μm (Figure S2a) were obtained, which is ascribed to the increment of concentration of TIPB-Cl and palladium acetate. Similarly, the decrement of concentration of TIPB-Cl and palladium acetate results in the formation of smaller spherical particles (Figure S2b).

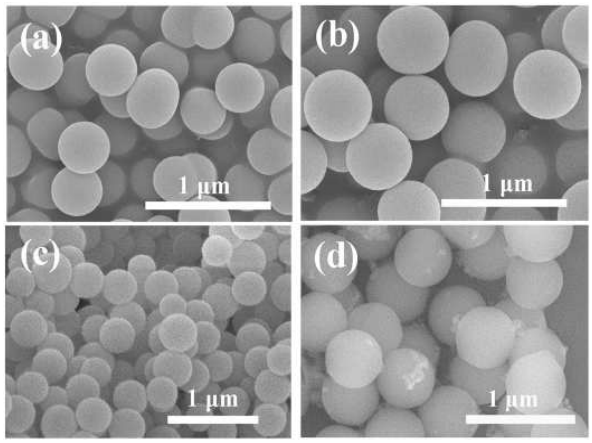

Figure 2. Typical SEM images of PNP1 (a), PNP2 (b), Fe_3O_4@PNP1 (c) and Fe_3O_4@PNP2 (d).

Interestingly, when toluene-dispersed Fe_3O_4 NPs were added into the mixture of TIPT-Cl or TIPB-Cl with 1.5 equivalent of palladium acetate, Fe_3O_4@PNP1 and Fe_3O_4@PNP2 were formed under the same conditions (Scheme 1), respectively. Fe_3O_4@PNP1 and Fe_3O_4@PNP2 are magnetically separable with the help of external magnetic field (Figure S3). TEM images has showed that Fe_3O_4 NPs are effectively encapsulated inside palladium NHC spheres as core, in which Fe_3O_4 NPs can be clearly distinguished (Figure 3).

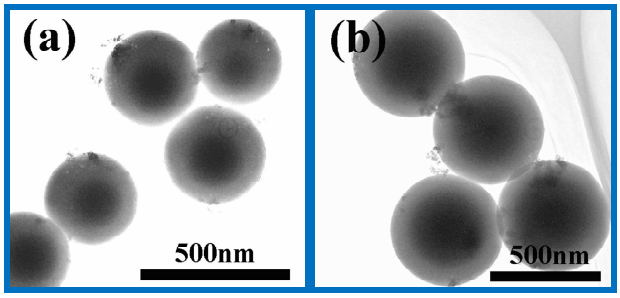

Figure 3. TEM images of Fe_3O_4@PNP1 (a) and Fe_3O_4@PNP2 (b).

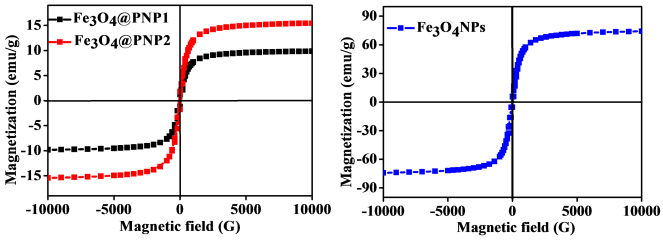

Figure 4. Field-dependent magnetization curves at 300K for Fe_3O_4@PNP1 and Fe_3O_4@PNP2 (left) and bare Fe_3O_4 NPs (right).

The magnetic properties of as-synthesized Fe_3O_4@PNP1 and Fe_3O_4@PNP2 were investigated at 300 K in the magnetic field ranging from -10 to +10 KOe. As shown in Figure 4, the absence of magnetic hysteresis suggests the superparamagnetic behavior of such magnetic core-shell particles. The saturation magnetization of Fe_3O_4@PNP1 and Fe_3O_4@PNP2 is smaller than that of bare Fe_3O_4 NPs due to the entrapment of Fe_3O_4 NPs into the main-chain palladium NHC polymers, but the magnetization is large enough for magnetic separation of the spherical particles (Figure S3). X-ray diffraction (XRD) patterns show that the characteristic peaks and relative intensities of Fe_3O_4@PNP1 and Fe_3O_4@PNP2 match well with that of bare Fe_3O_4 NPs (Figure S4), which indicates that the particles encapsulated into main-chain palladium NHC polymers are the original Fe_3O_4 NPs, and the encapsulation process does not modify the nature of the embedded materials.[8c]

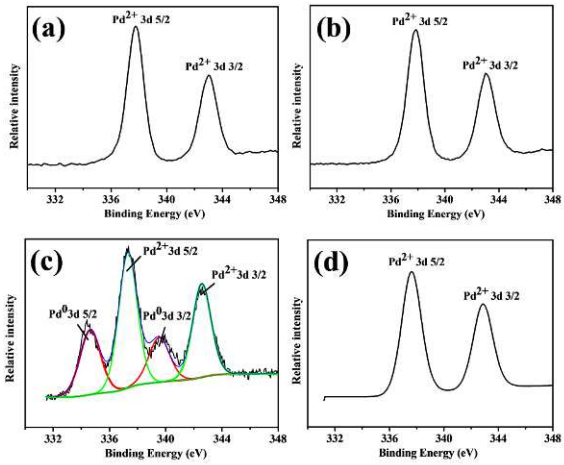

Figure 5. XPS spectra of palladium for Fe_3O_4@PNP1 (a), Fe_3O_4@PNP2 (b), Fe_3O_4@PNP1-6run (c) and Fe_3O_4@PNP2-6run (d).

All of the particles are insoluble in DMF and common organic solvents. The formation of main-chain palladium NHCs as shell of Fe_3O_4@PNP1 and Fe_3O_4@PNP2 is confirmed by solid-state ^{13}C NMR, IR and TG-MS and XPS analyses. The solid-state ^{13}C NMR spectra of Fe_3O_4@PNP1 and Fe_3O_4@PNP2 are nearly similar to each other except for the peak at 170 ppm in Fe_3O_4@PNP2 (Figure S5), which is assigned as carbon atoms of triazine ring. The peaks at 155-166 ppm are assigned as carbene carbon atoms, clearly confirming the formation of palladium NHC species. The peaks at 39 and 55 ppm correspond to methyl group and methylene group, respectively. The remaining peaks at 127-142 ppm are attributed to carbon atoms of phenyl and imidazolyl rings. In comparison with IR spectra of TIPT-Cl and TIPB-Cl, the strong band of quaternary imidazolium at 1165 cm^{-1} decreases sharply, while the new band at 1236 cm^{-1} appears in IR spectra of Fe_3O_4@PNP1 and Fe_3O_4@PNP2 (Figure S6), further suggesting successful conversion from imidazolium salts to palladium NHCs. TG-MS analyses show that both Fe_3O_4@PNP1 and Fe_3O_4@PNP2 are stable up to 250 °C. Initial weight losses of 2.3% in Fe_3O_4@PNP1 and 4.7% in Fe_3O_4@PNP2 before 110 °C are mainly ascribed to the presence of water

molecules captured by the particles, which is confirmed by ion current at m/z = 18. Subsequent weight losses of 9.7% and 5.3% at 110-250 °C correspond to removal of DMF with ion current at m/z = 73 (Figure S7). ICP analyses show that palladium contents in Fe_3O_4@PNP1 and Fe_3O_4@PNP2 are 1.07 and 0.82 mmol/g, respectively. In palladium XPS spectra, Fe_3O_4@PNP1 and Fe_3O_4@PNP2, only show the peaks of Pd(II) binding energy at 337.8 eV (Pd $3d_{5/2}$) and 343.0 eV (Pd $3d_{3/2}$) (Figure 5), suggesting surface palladium(II) is not reduction during the preparation of the magnetic core-shell particles. In comparison with Pd $3d_{5/2}$ peak of free $Pd(OAc)_2$ at 338.4 eV,[15] the negative shift of the peak about 0.6 eV further collaborates the formation of main-chain palladium NHC polymers. TEM elementary mapping experiments reveal homogeneous distribution of carbon, nitrogen, palladium and chloride in a wide region in Fe_3O_4@PNP1 and Fe_3O_4@PNP2 (Figure 6).

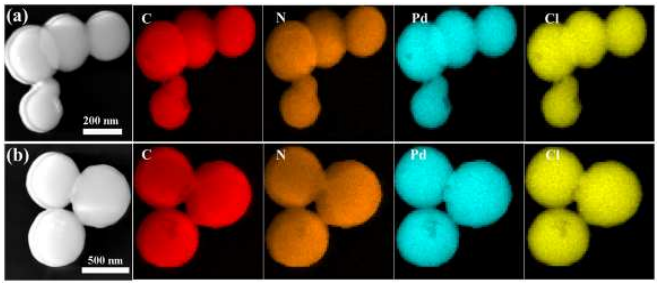

Figure 6. High-annular dark-field scanning TEM (HAADF-STEM) images and elementary mapped images of C, N, Pd and Cl in Fe_3O_4@PNP1 (a) and Fe_3O_4@PNP2 (b).

The catalytic performances of the palladium NHC particles were investigated in palladium-catalyzed Suzuki-Miyaura coupling reaction. When the reaction between 4-bromoacetophenone and phenylboronic acid was performed using Fe_3O_4@PNP1 as a precatalyst in the presence of K_2CO_3 in H_2O/EtOH at 25 °C for 1 h, 4-acetylbiphenyl was obtained in a quantitative GC yield, while Fe_3O_4@PNP2 gave a 92% GC yield. It should be mentioned that this catalytic activity is challenging to achieve at 25 °C even for homogeneous catalytic systems.[6e] The magnetic palladium NHC particles were easily separated by a permanent magnet after the catalytic reaction. However, when PNP-1 and PNP-2 were used as precatalysts under the same conditions, GC yields of 95 and 85% were obtained, respectively (Figure S8), which are lower than those from their corresponding magnetic counterparts.

Stability and reusability are very important factors for a heterogeneous catalytic system. The good catalytic activity and easy magnetic separation of Fe_3O_4@PNP1 and Fe_3O_4@PNP2 encourage us to investigate their recyclability. After the completion of the reaction between 4-bromoacetophenone and phenylboronic acid, the crude product was extracted with ethyl acetate, and followed by the addition of acetone to reduce viscosity of catalytic systems. The palladium NHC particles were separated by a permanent magnet, washed with H_2O, acetone and diethyl ether, and reused for the next run. Interestingly, Fe_3O_4@PNP2 can be used at least 6 times without significant loss of catalytic activity (Figure 7), while catalytic activity of Fe_3O_4@PNP1 gradually decreases, especially after three consecutive runs. The distinction is probably ascribed to the difference of the conjugated effect between triphenyltriazine and triphenylbenzene. It is known that the cycle of Pd(0) and Pd(II) species is usually involved in Suzuki-Miyaura coupling reaction. In Fe_3O_4@PNP1, the effective conjugation of triazine ring with the adjacent phenyl rings inhibits the free rotation of TIPT-Cl (Scheme 1), resulting in inefficient capture of the active Pd(0) species and restoration of Pd(II) NHC species, while for Fe_3O_4@PNP2, the bonds between phenyl rings in TIPB-Cl can rotate freely to help TIPB-Cl capture the metastable palladium species adaptively and restore to Pd(II) NHC species. As a result, Fe_3O_4@PNP2 shows a much more prominent recyclability than Fe_3O_4@PNP1, although Fe_3O_4@PNP1 exhibits a slightly higher catalytic activity in the first run. The catalytic activity in Fe_3O_4@PNP1 gradually drops in subsequent runs. The observations were further confirmed by XPS analyses of Fe_3O_4@PNP1 and Fe_3O_4@PNP2 after six consecutive runs (denoted as Fe_3O_4@PNP1-6run and Fe_3O_4@PNP2-6 run, respectively). As shown in Figure 5, Pd(0) species were observed in Fe_3O_4@PNP1-6 run, the ratio of Pd(II)/Pd(0), which is estimated by their ratio of relative peak areas, is 1.88. Unexpectedly, only Pd(II) is detected in Fe_3O_4@PNP2-6run, their peaks of binding energy are

identical with Fe_3O_4@PNP2. Notably, Fe_3O_4@PNP1 and Fe_3O_4@PNP2 still remain original spherical morphologies after six successive runs (Figure 8), which is probably attributed to mild reaction conditions and facilely magnetic separation of catalysts.

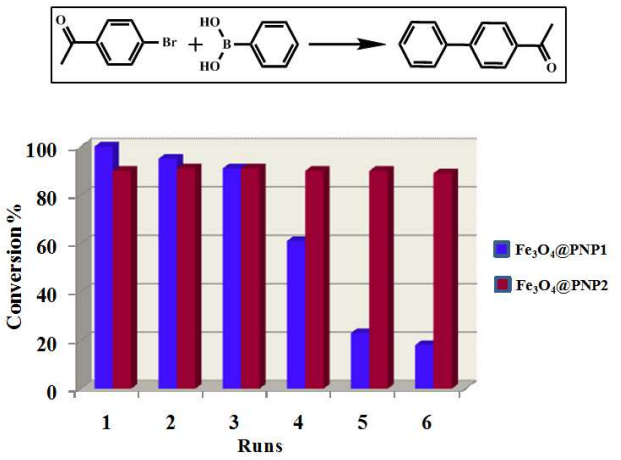

Figure 7. Recyclability of Fe_3O_4@PNP1 and Fe_3O_4@PNP2 in Suzuki-Miyaura cross-coupling reaction at 25 °C. Reaction conditions: 4-bromoacetophenone (2.0 mmol), phenylboronic acid (3.0 mmol), K_2CO_3 (4.0 mmol) and [Pd] in Fe_3O_4@PNP1 or Fe_3O_4@PNP2 (1.0 mol%) in water (4.0 mL) and EtOH (8.0 mL) at 25 °C for 1 h.

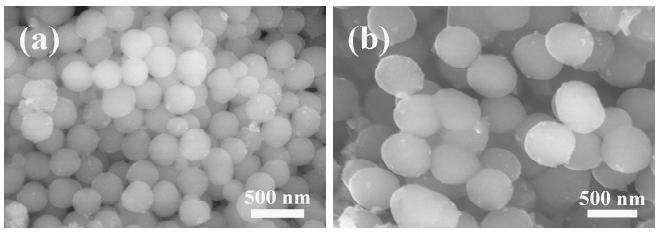

Figure 8. Typical SEM images of Fe_3O_4@PNP1-6run (a) and Fe_3O_4@PNP2-6run (b)

Conclusions

A facile method for the synthesis of the spherical core-shell palladium NHC particles were presented using magnetite NPs as core and main-chain palladium NHC particles as shell. The magnetic organometallic particles not only are readily separable after catalytic reaction using an external magnet, but also show high catalytic activity in Suzuki-Miyaura coupling reaction at 25 °C, which is challenging to achieve even for homogeneous catalytic systems. It should be mentioned that the morphologies of the spherical particles have no significant variation after the catalytic systems were used six times, which are much different from most of the reported spherical particles in liquid-phase catalytic reactions. In addition, Fe_3O_4@PNP2 shows better recyclability than Fe_3O_4@PNP1, and only Pd(II) is observed after six consecutive runs, while Pd(0) and Pd(II) coexist in Fe_3O_4@PNP1 under the same conditions, which results from the difference of the conjugated effect between triphenyltriazine and triphenylbenzene from main-chain palladium NHC shell. In summary, this study not only offers a new strategy for the construction of magnetic core-shell organometallic particles through facile encapsulation, but also greatly widens the scope of palladium NHC polymers.

Acknowledgements

The authors acknowledge State Key Project of Fundamental Research for Nanoscience and Nanotechnology (2011CBA00502) and National Natural Science Foundation of China (21273239, 21471151) for financial support.

Notes and references

[a] State Key Laboratory of Structural Chemistry, Fujian Institute of Research on the Structure of Matter, Chinese Academy of Sciences, Fuzhou, Fujian, 350002, China. E-mail: ruihu@fjirsm.ac.cn
[b] University of Chinese Academy of Sciences, Beijing, 100049, China.
Electronic Supplementary Information (ESI) available: the additional SEM images, IR spectra, TG-MS curves, Solid state ^{13}C NMR spectra, XPS spectra and XRD spectra of palladium NHC particles. See DOI: 10.1039/b000000x/.

1. a) M. Sanlés-Sobrido, M. Pérez-Lorenzo, B. Rodríguez-González, V. Salgueiriño, M. A. Correa-Duarte, *Angew. Chem. Int. Ed.* 2012, **51**, 3877-3882; b) T. Lu, X. Li, L. Gu, Y. Zhang, *ChemSusChem* 2014, **7,** 2423-2426; c) K. H. Park, I. Ku, H. J. Kim, S. U. Son, *Chem. Mater.* 2008, **20**, 1673-1675.
2. a) H. Yu, X. Qiu, S. P. Nunes, K. V. Peinemann, *Nat Commun* 2014, **5**, 4110; b) S. Cao, L. Fang, Z. Zhao, Y. Ge, S. Piletsky, A. P. F. Turner, *Adv. Funct. Mater.* 2013, **23**, 2162-2167; c) X. Zhu, P. C. Hillesheim, S.

M. Mahurin, C. Wang, C. Tian, S. Brown, H. Luo, G. M. Veith, K. S. Han, E. W. Hagaman, H. Liu, S. Dai, *ChemSusChem* 2012, **5**, 1912-1917.

3. a) J. C. Park, J. Y. Kim, E. Heo, K. H. Park, H. Song, *Langmuir* 2010, **26**, 16469-16473; b) F. Caruso, M. Spasova, A. Susha, M. Giersig, R. A. Caruso, *Chem. Mater.* 2001, **13**, 109-116; c) B. Lim, J. Jin, J. Yoo, S. Y. Han, K. Kim, S. Kang, N. Park, S. M. Lee, H. J. Kim , S. U. Son, *Chem. Commun.* 2014, **50**, 7723-7726; d) I. Imaz, D. Maspoch, C. Rodríguez-Blanco, J. M. Pérez-Falcón, J. Campo, D. Ruiz-Molina, *Angew. Chem. Int. Ed.* 2008, **47,** 1857-1860.
4. a) M. Oh, C. A. Mirkin, *Angew. Chem. Int. Ed.* 2006, **45,** 5492-5494; b) Y. M. Jeon, G. S. Armatas, J. Heo, M. G. Kanatzidis, C. A. Mirkin, *Adv. Mater.* 2008, **20,** 2105-2110; c) F. Ke, L. G. Qiu, J. Zhu, *Nanoscale* 2014, 6, 1596-1601; d) J. Zhuang, C. H. Kuo, L. Y. Chou, D. Y. Liu, E. Weerapana, C. K. Tsung, *ACS Nano* 2014, **8**, 2812-2819.
5. a) G. C. Fortman, S. P. Nolan, *Chem Soc Rev.* 2011, **40**, 5151-5169; b) K. V. S. Ranganath, J. Kloesges, A. H. Schafer, F. Glorius, *Angew. Chem. Int. Ed.* 2010, **49**, 7786-7789; c) K. V. S. Ranganath, S. Onitsuka, A. K. Kumar, J. Inanaga, *Catal. Sci. Technol.* 2013, **3**, 2161-2181; d) M. N. Hopkinson, C. Richter, M. Schedler, F. Glorius, *Nature* 2014, **510**, 485-496; e) S. Gonell, M. Poyatos, E. Peris, *Chem. Eur. J.* 2014, **20**, 5746-5751 .
6. a) A. J. Boydston, K. A. Williams, C. W. Bielawski, *J. Am. Chem. Soc.* 2005, **127**, 12496-12497; b) J. Choi, H. Y. Yang, H. J. Kim, S. U. Son, *Angew. Chem. Int. Ed.* 2010, **49**, 7718-7722; c) C. Zhang, J. J. Wang, Y. Liu, H. Ma, X. L. Yang, H. B. Xu, *Chem. Eur. J.* 2013, **19**, 5004-5008; d) B. Karimi, P. F. Akhavan, *Inorg. Chem.* 2011, **50**, 6063-6072; e) B. Karimi, P. F. Akhavan, *Chem. Commun.* 2011, **47**, 7686-7688.
7. a) M. B. Gawande, P. S. Brancoa, R. S. Varma, *Chem. Soc. Rev. 2013, **42***, 337-**133**93; b) M. Kim, J. C. Park, A. Kim, K. H. Park, H. Song, *Langmuir, 2012, **28**, 6441-64*47; c) **S**. Sá, M. B. Gawande, A. Velhinho, J. P. Veiga, N. Bundaleski, J. Trigueiro, *A. Tolstogou*zov, O**. M**. N. D. Teodoro, R. Zboril, R. S. Varma, P. *S. Branco, Green **Ch**em.* 2014, **16** , 3494-3500.
8. a) V. Polshettiw*ar, R. Luque,* A. Fi**hri**, H. Zhu, M. Bouhrara, J. M. Basset, *Chem. Rev.* 2011, **111,** *3036-3075; b)* R. B. **N.** Baig , R. S. Varma, *Chem. Commun.* 2013, **49**, 752-770; c) A. Pourj*avadi, S.* H. Ho**sse**ini, M. Doulabi, S. M. Fakoorpoor, F. Seidi, *ACS Catal.* 2012, **2**, 1259-1266.
9. a) A. H. Lu, E. L. Salabas, F. Schuth, *Angew. Chem. Int. Ed.* 2007, **46**, 1222-1244; b) A. Saha, *J. Leazer,* R. S. **Va**rma, *Green Chem.* 2012, **14**, 67-71; c) P. D. Stevens, G. Li, J. Fan, M. Yen, Y. Gao, *Chem. Commun.* 2005, 4435-4437; d) Y. Zheng, P. D. Stevens, Y. Gao, *J. Org. Chem.* 2006, **71**, 537-542.
10. a) R. Ricco, L. Malfatti, M. Takahashi, A. J. Hill, P. Falcaro, *J. Mater. Chem. A* 2013, **1**, 13033-13045; b) Y. Liao, L. He, J. Huang, J. Zhang, L. Zhuang, H. Shen, C. Y. Su, *ACS Appl. Mater. Interfaces* 2010, **2**, 2333-2338; c) P. Agrigento, M. J. Beier, J. T. N. Knijnenburg, A. Baiker, M. Gruttadauria, *J. Mater. Chem.* 2012, **22**, 20728-20735.
11. a) I. Imaz, J. Hernando, D. Ruiz-Molina, D. Maspoch, *Angew. Chem. Int. Ed.* 2009, **48**, 2325-2329; b) P. D. Stevens, J. Fan, H. M. R. Gardimalla, M. Yen, Y. Gao, *Org. Lett.* 2005, **7**, 2085-2088.
12. a) H. Zhao, Y. Wang, R. Wang, *Chem. Commun.* 2014, **50**, 10871-10874; b) L. Li, H. Zhao, J. Wang, R. Wang, *ACS Nano* 2014, **8**, 5352-5364; c) H. Zhao, L. Li, Y. Wang, R. Wang, *Sci. Rep.* 2014, **4**, 5478; d) L. Li, Z. Chen, H. Zhong, R. Wang, *Chem. Eur. J.* 2014, **20**, 3050-3060.
13. Y. Zhang, L. Zhao, P. K. Patra, D. Hu, J. Y. Ying, *Nano Today* 2009, **4**, 13-20.
14. a) D. Sun, S. Ma, Y. Ke, T. M. Petersen, H. C. Zhou, *Chem. Commun.* 2005, 2663-2665; b) Y. R. Liu, L. He, J. Zhang, X. Wang, C. Y. Su, *Chem. Mater.* 2009, **21**, 557-563.
15. S. Y. Ding, J. Gao, Q. Wang, Y. Zhang, W. G. Song, C. Y. Su, W. Wang, *J. Am. Chem. Soc.* 2011, **133,** 19816-19822.
16. a) X. L. Zhang, C. P. Guo, Q. Y. Yang, W. Wang, W. S. Liu, B. S. Kang, C. Y. Su, *Chem. Commun.* 2007, **41**, 4242-4244; b) A. Garcia, B. Insuasty, M. A. Herranz, R. Martinez-Alvarez, N. Martin, *Org. Lett.* 2009, **11,** 5398-5401.
17. J. D. Badjić, S. J. Cantrill, J. F. Stoddart, *J. Am. Chem. Soc.* 2004, **126**, 2288-2289.
18. M. J. Frisch, G. W. Trucks, H. B. Schlegel, G. E. Scuseria, M. A. Robb, J. R. Cheeseman, J. A. Montgomery, Jr., T. Vreven, K. N. Kudin, J. C. Burant, J. M. Millam, S. S. Iyengar, J. Tomasi, V. Barone, B. Mennucci, M. Cossi, G. Scalmani, N. Rega, G. A. Petersson, H. Nakatsuji, M. Hada, M. Ehara, K. Toyota, R. Fukuda, J. Hasegawa, M. Ishida, T. Nakajima,

Y. Honda, O. Kitao, H. Nakai, M. Klene, X. Li, J. E. Knox, H. P. Hratchian, J. B. Cross, V. Bakken, C. Adamo, J. Jaramillo, R. Gomperts, R. E. Stratmann, O. Yazyev, A. J. Austin, R. Cammi, C. Pomelli, J. W. Ochterski, P. Y. Ayala, K. Morokuma, G. A. Voth, P. Salvador, J. J. Dannenberg, V. G. Zakrzewski, S. Dapprich, A. D. Daniels, M. C. Strain, O. Farkas, D. K. Malick, A. D. Rabuck, K. Raghavachari, J. B. Foresman, J. V. Ortiz, Q. Cui, A. G. Baboul, S. Clifford, J. Cioslowski, B. B. Stefanov, G. Liu, A. Liashenko, P. Piskorz, I. Komaromi, R. L. Martin, D. J. Fox, T. Keith, M. A. Al-Laham, C. Y. Peng, A. Nanayakkara, M. Challacombe, P. M. W. Gill, B. Johnson, W. Chen, M. W. Wong, C. Gonzalez, and J. A. Pople, Gaussian, Inc., Wallingford CT, 2004.

19. a) C. T. Lee, W. T. Yang, R. G. Parr, Phys. Rev. B 1988, 37, 785-789; b) A. D. Becke, *J. Chem. Phys.* 1993, **98,** 5648-5652.

20. a) A. E. Reed, F. Weinhold, *J. Chem. Phys.* 1983, **78,** 4066-4073; b) A. E. Reed, R. B. Weinstock, F. Weinhold, *J. Chem. Phys.* 1985, **83,** 735-746; c) A. E. Reed, L. A. Curtiss and F. Weinhold, *Chem. Rev.* 1988, **88,** 899-926.